









Research Article

Permeability Enhancement Technology for Soft and Low-Permeability Coal Seams Combined with Hydraulic Perforation and Hydraulic Fracturing

Zhengjie Shang ^{1,2}, Zhaofeng Wang ^{1,3}, Zhiheng Cheng ⁴, Hongbing Wang ⁵,
Liang Chen ⁴, Lei Li ^{1,6}, Jianhua Fu ^{1,2} and Hao Liu ⁷

¹School of Safety Science and Engineering, Henan Polytechnic University, Jiaozuo, Henan, China 454003

²Zhengzhou Coal Industry (Group) Co., Ltd., Henan, China 450007

³Coal Mine Disaster Prevention and Disaster Relief Engineering Research Center of the Ministry of Education, Jiaozuo, China 454003

⁴North China Institute of Science and Technology, China 065201

⁵School of Civil and Resource Engineering University of Science and Technology Beijing, China 100083

⁶Institute of Industrial Technology, Henan Polytechnic University Jiaozuo, Henan, China 454003

⁷College of Aerospace Engineering, Chongqing University, Chongqing, China 400044

Correspondence should be addressed to Zhiheng Cheng; zh_cheng_2021@126.com and Hao Liu; liuhaocqu@cqu.edu.cn

Received 4 April 2022; Accepted 27 June 2022; Published 15 July 2022

Academic Editor: Xiangguo Kong

Copyright © 2022 Zhengjie Shang et al. This is an open access article distributed under the Creative Commons Attribution License, which permits unrestricted use, distribution, and reproduction in any medium, provided the original work is properly cited.

The No. 2₁ coal seam in the Zhengzhou mining area is a soft, three-layer, low-permeability coal seam prone to outbursts. The three-layer structure includes the coal seam and the roof and floor layers, which exhibit high gas contents and poor permeability. The dynamic hazards caused by coal and gas outbursts are very serious. A new permeability-increasing fracturing technique that combines hydraulic perforation and hydraulic fracturing was developed specifically for the geologic conditions of the gas-bearing No. 2₁ coal seam. Numerical simulations were developed to study the influence of the technique on the stress distribution and permeability of the coal around the borehole. In addition, the extracted borehole gas concentrations and extraction amounts at multiple sites were investigated before and after using the technique. The study shows that the permeability-increasing fracturing technique destroys the concentrated stress coal pillars via the development of fractures between boreholes in exposed hydraulically perforated coal. The coal stress within the zone with an effective increase in permeability decreased by 30%. Furthermore, the permeability in this zone increased by three times, and the average extracted gas concentration increased by over six times. The gas pressure in the No. 2₁ coal seam decreased from 1.1 MPa to 0.4 MPa, and the gas content decreased from 15.96 m³/t to 5.6 m³/t. All outburst prediction indexes measured on site did not exceed their respective limits. The technique not only effectively eliminated the dynamic hazards caused by coal and gas outbursts but also achieved efficient gas extraction in the Zhengzhou mining area.

1. Introduction

The coal and gas outburst dynamics are the result of the combined effects of ground stress, gas pressure, and coal mechanical properties [1–6]; it always threatens the safety of underground production as a serious mine disaster [7–12]. In some soft outburst coal seams with low permeability in China,

the coal seam has suffered from strong structural compression deformation due to the influence of multistage geological structure, and its primary structure has been damaged seriously, and the coal body strength and coal seam permeability are low [13–17]. Therefore, the dynamic disaster of coal and gas outburst in this kind of coal seam is very serious, and with the deepening of the mining gradient, the mining conditions of

the soft outburst coal seam under high ground stress, high gas pressure, and low permeability will become more worse [18–21]. Coal and gas outburst dynamic disasters are also increasingly threatening mine safety production [22, 23]. However, it is difficult to eliminate the danger of coal seam outburst relying on the traditional prevention and control measures such as optimizing the coal seam gas drainage technology (reducing the borehole spacing, increasing the number of boreholes, and prolonging the drainage time) [24–26] or coal seam pressure relief mining.

The permeability of coal seam is an important index to measure the gas drainage ability of coal seam. For low-permeability coal seams, especially low-permeability soft outburst coal seams, this indicator will directly affect the outburst prevention and elimination effect of coal seams, such as the literature [27] utilizing the laboratory test method, the path control effects of CBM migration characteristics in coal reservoirs were studied, and mechanisms of CBM migration in coal reservoirs were analyzed and discussed. Therefore, special measures must be taken to improve the permeability of coal seam [28]. At present, many scholars at home and abroad have carried out a lot of research on increasing coal seam permeability (or rapid outburst elimination technology) under soft outburst coal seam with low permeability. For example, the pressure relief and permeability enhancement technology of protective layer is to increase the permeability of the underlying coal seam by mining the upper protective layer in the low-permeability coal seam, so as to improve the gas drainage rate of the low-permeability coal seam and reduce the risk of gas outburst in the working face [29–31]. Literature [32] discusses the coupling relationship between fractures in overlying strata and gas seepage fields for pressure relief during mining of outburst-prone coal seam groups to quantitatively characterize the distribution characteristics of favorable areas for coalbed methane (CBM) drainage in mining-induced fractures of overlying strata. And literature [33] bases on the production experience of coal mines and the summaries of experts; a production deployment evaluation system with eleven indices for outburst-prone coal mines is established; CO₂ phase change fracturing and permeability enhancement technology is to inject high concentration of CO₂ into the body by high pressure to achieve phase change fracturing of broken coal-rock mass, thus increasing the permeability of coal and rock [34–36]. Deep hole blasting fracturing and permeability-increasing technology is to produce explosion shock wave in the borehole to fracture surrounding coal and rock, so as to achieve the purpose of permeability enhancement [37, 38]. The technology of freeze fracturing permeability enhancement is to increase the seepage rate of coal reservoir by rapidly reducing the temperature of coal and rock mass and then changing the pore structure of coal reservoir [39]. However, this technology is still in the stage of laboratory research and cannot be used in large-scale underground. The technology of hydraulic perforation pressure relief and permeability enhancement is to release the coal body through the scouring effect of water flow, which reduces the stress of coal seam, increases the permeability, and releases the coal seam gas, thus eliminating the danger of coal seam outburst [40–42], and the experimental system established in reference

[43] reveals the fluid solid coupling property of gas-bearing coal subjected to hydraulic slotting. The technology of hydraulic fracturing permeability enhancement is to inject high-pressure water into the coal seam boreholes; under the pressure, the coal body around the borehole appears cutting cracks; and with the continuous injection of high-pressure water, the cracks gradually extend to the depth of the borehole, thus increasing the coal seam permeability [44, 45]. Literature [46] explored the change rule of the compressive strength, elastic modulus, and Poisson's ratio of slotted coal samples with the slotting angle and found that the change rule, respectively, conforms to the Boltzmann function, logistic function, and quadratic function.

To sum up, the various coal seam permeability enhancement technologies studied by predecessors all start from changing the external pressure of coal seam, through causing coal body pressure relief and uneven deformation and damage, opening the original cracks, generating new cracks, and connecting the cracks with each other, so as to provide channels for gas desorption and flow. These technical measures have played a greater role in promoting the permeability of coal seam. However, there are still many problems if only a single coal seam permeability enhancement technology is used in practical engineering application. For example, a single low-permeability outburst coal seam does not have the conditions for mining protective layer. When the technology of hydraulic perforation pressure relief and permeability enhancement is adopted, pores of varying sizes and concentrated stress coal pillars appear in the process of coal tunnel excavation, which not only makes the support of coal tunnel difficult but also makes the stress distribution of coal body uneven, and under the action of excavation stress, the hole will suddenly collapse, causing abnormal gas emission from the coal seam. When the hydraulic fracturing technology is adopted, the gas drainage rate of coal seam drilling often has the problem of too fast attenuation rate.

Therefore, the author based on the limitations of various single coal seam permeability enhancement technology, taking the Zhengzhou Gaocheng mine as the research object and creatively puts forward a new permeability-increasing technique combining hydraulic perforation and hydraulic fracturing. The technology is to set hydraulic perforation boreholes between coal uncovering boreholes based on coal uncovering caused by hydraulic fracturing thus to eliminate the stress-concentrated coal pillars between coal uncovering boreholes, realize uniform stress distribution of coal, and widely improve permeability of coal.

2. Permeability-Increasing Hydraulic Technique

Hydraulic perforation involves drilling holes in the construction layer of a floor roadway. A water jet is used in the crossing holes. The coal is dislodged by the scouring action of the water flow. Therefore, the advantages of hydraulic perforation are shown below. The process of hydraulic perforation reduces coal seam stress, increases permeability, releases gas, and eliminates the outburst hazard of the coal seam. The principles of the permeability-increasing technique are as follows: during

the drilling process of the hydraulic perforation bits, coal is partially crushed under the effect of the water jet and bit cutting, which encourages the release of coal stress and reduces the potential for gas expansion. Under the effects of the water flow, crushed coal and gas are released into the borehole, thereby releasing the coal stress and gas pressure. Due to creep deformation in the coal, the permeability of the coal increases correspondingly. A schematic drawing of hydraulic perforation system is shown in Figure 1.

Permeability-increasing hydraulic fracturing utilizes a high-pressure pump to inject highly pressurized water into boreholes with a displacement far greater than the absorption capacity of the coal seam. After borehole sealing, the highly pressurized water imposes a pressure exceeding the stress around the pore wall and the tensile strength of the coal-rock mass, and cracks form in the coal seam. As liquid is continuously injected into the cracks, the cracks gradually extend away from the borehole. The fracturing fluid is discharged after the fracturing process is completed. Therefore, the advantages of hydraulic fracturing are shown below. Hydraulic fracturing has formed a channel for gas flow, improving the permeability of the coal seam, reducing the amount of drilling necessary, improving the gas extraction rate, and shortening the extraction duration. In addition, hydraulic fracturing promotes uniform stress distribution within the coal, thus eliminating the local stress concentration caused by the geologic structure. Moreover, coal moisture increases, and dust concentrations decrease. A schematic drawing of hydraulic fracturing is shown in Figure 2.

Permeability-increasing fracturing technique that combines hydraulic perforation of exposed coal and hydraulic fracturing involves the comprehensive application of both hydraulic perforation and hydraulic fracturing. During the application of hydraulic perforation measures to exposed coal in crossing holes, holes form within the coal. Under the joint action of geostatic stress and gas, the coal is subject to creep deformation, and the stress distribution is rearranged. The coal stress around the borehole decreases, and the coal permeability increases. However, after the implementation of hydraulic perforation, uncovered holes in the coal form. The coal pillar stress between the holes increases and the permeability decreases, which reduces the migration of coal gas to the boreholes. Hydraulic perforation holes increase the probability of abnormal gas emissions, which represent a hazard factor for the safe construction of coal roadways. In addition, because boreholes in a soft coal seam are prone to collapse and duct blockage, hydraulic perforation measures do not relieve the pressure conditions or enhance permeability over large areas in a coal seam. To eliminate the pillars of concentrated stress between the uncovered hydraulic perforation holes, promote creep deformation in the coal, rearrange the stress, and eliminate the residual boreholes, it is necessary to create hydraulic fracturing holes. The fracturing effects of injecting highly pressurized water into the coal promotes weak plane expansion, crack extension, formation of a connected fracture network within a certain volume, and gas desorption from the coal as the gas migrates to the extraction drilling channel. These processes result in a large area of uniform pressure relief and a permeability increase in the coal seam. Therefore, it is necessary to com-

bine both hydraulic perforation and hydraulic fracturing. The working principle and drilling layout of hydraulic flushing coal drainage and fracturing coupling fracturing and permeability enhancement in Gaocheng mine of Zhengzhou mining area are shown in Figures 3 and 4.

3. Numerical Simulation Analysis of Coupled Hydraulic Perforation and Fracturing

3.1. Numerical Simulation Scheme and Model Parameters. According to the drilling data of the 25091 floor roadway in the Zhengzhou Gaocheng mine, the No. 2₁ coal seam is 6 m thick. The top layer of the coal seam is a 6 m thick siltstone. The floor layer is a 6 m thick sandy mudstone. The rate of coal uncovering caused by hydraulic perforation in the Gaocheng mine is 30%. The diameter of the zone influenced by hydraulic perforation is 0.6 m. The water pressure for the hydraulic fracturing is 20 MPa. To analyze the impact of the multiple drill holes for hydraulic perforation and hydraulic fracturing on coal stress and permeability, the simulation analyzed 9 drill holes. The drill hole spacing was 6 m, and the drill holes traversed the coal seam. After completing the hydraulic perforation process, the coal stress returned to equilibrium. We selected the middle drill hole and injected water at 20 MPa to hydraulically fracture the coal. To reduce the influence of the model boundary effect, we retained 9 m thick coal pillars around the drill hole. The physical and mechanical parameters of the No. 2₁ coal seam, as well as those of the roof and floor layers, are shown in Table 1. We set the inclination angle of the coal-rock layer in the numerical model to 0° and the thicknesses of the coal seam and the roof and floor layers to 6 m, and we applied 5 MPa of vertical stress to the top of the model. The drill hole layout of the numerical simulation scheme is shown in Figure 5.

3.2. Numerical Simulation Results of Coal Uncovering via Hydraulic Perforation

3.2.1. Analysis of Hydraulic Fracturing Stress Field. Before drilling of the construction layer of the floor roadway, the coal stress should be less than the initial equilibrium condition. Vertical stress should be directly related to burial depth. After coal uncovering caused by hydraulic perforation, the coal stress within a certain distance around a drill hole is reduced. The coal then generates creep deformation, cracks increase, and the coal permeability improves. To analyze the coal stress field distribution around a drill hole after coal uncovering caused by hydraulic perforation, we extracted a horizontal profile along $z = 9$ m and a vertical profile along $x = 15$ m in the numerical model to obtain a coal stress field distribution diagram. The stress field distribution diagram of the horizontal and vertical profiles after hydraulic perforation is shown in Figure 6.

The figure shows the following three points. (1) The coal stress around the boreholes is significantly reduced after implementing coal uncovering measures using hydraulic perforation. The pressure relief range also increases. In addition, the zones of stress reduction surrounding the drill holes are connected, which indicates that the coal uncovering

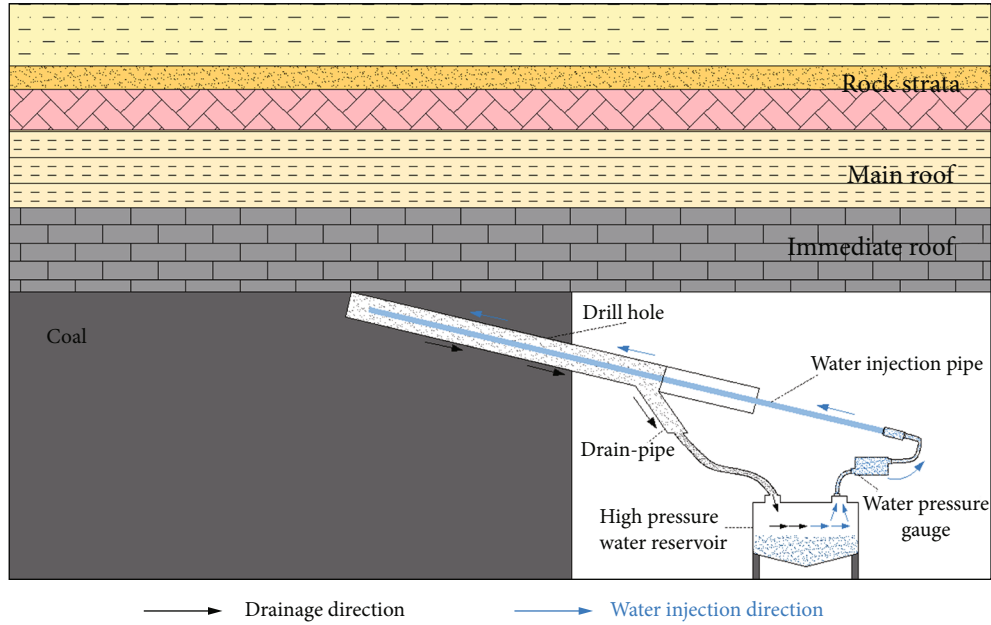


FIGURE 1: Schematic drawing of hydraulic perforation.

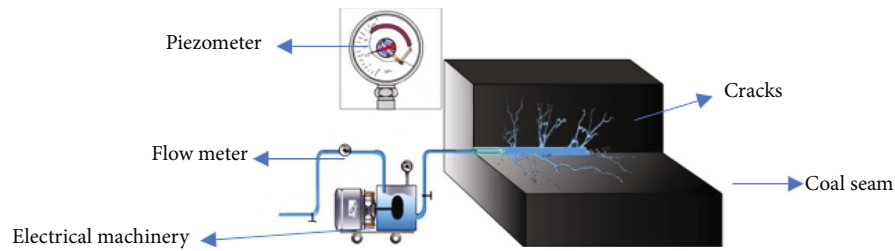


FIGURE 2: Schematic drawing of hydraulic fracturing.

caused by multiple hydraulic perforation generates a synergistic permeability increase effect. (2) The zone of coal-rock mass stress reduction is greatest around the roof and floor layers of the borehole section. (3) The coal stress value within a distance of 0.8 m between boreholes is relatively high and is obviously higher than the coal stress around the other sites, which indicates that coal uncovering via hydraulic perforation between drill holes forms pillars of concentrated stress in the coal.

3.2.2. Permeability Evolution. To analyze coal permeability changes around a drill hole after coal uncovering caused by hydraulic perforation, we extracted a horizontal profile along $z = 9$ m and a vertical profile along $x = 15$ m in the numerical model to obtain a diagram of the permeability changes around the drill holes. The permeability changes in the horizontal and vertical profiles after hydraulic perforation are shown in Figure 7.

The figure shows the following three points. (1) The coal permeability around the boreholes has obviously increased, which indicates that the coal uncovering via hydraulic perforation improves the coal permeability. (2) The coal permeability within a distance of 3 m around the coal uncovering borehole increased due to the hydraulic fracturing. The

zones of increased permeability around each borehole intersect, which indicates coal crack communication between drill holes. (3) The coal permeability within 0.8 m of 4 boreholes is low, which indicates that coal uncovering caused by hydraulic perforation is prone to forming concentrated stress coal pillars. To realize a large area of pressure relief and increased permeability in a coal seam, further hydraulic fracturing measures should be performed.

3.3. Impact of Coupled Hydraulic Perforation and Fracturing on Seam Permeability. After performing hydraulic perforation, the stress becomes concentrated in the coal between the boreholes. If the borehole spacing is too large, concentrated stress pillars will be generated in the coal around the hydraulic perforation holes. Low coal permeability is detrimental to gas extraction. Therefore, in addition to hydraulic perforation, hydraulic fracturing measures must be taken. The concentrated stress coal pillars between the drill holes promote creep deformation, and the formation of a crack network results in a pressure release and increased permeability in a large area of coal.

3.3.1. Stress Field Distribution. Figure 8 shows that after performing hydraulic perforation and hydraulic fracturing, the following observations can be made regarding the coal stress

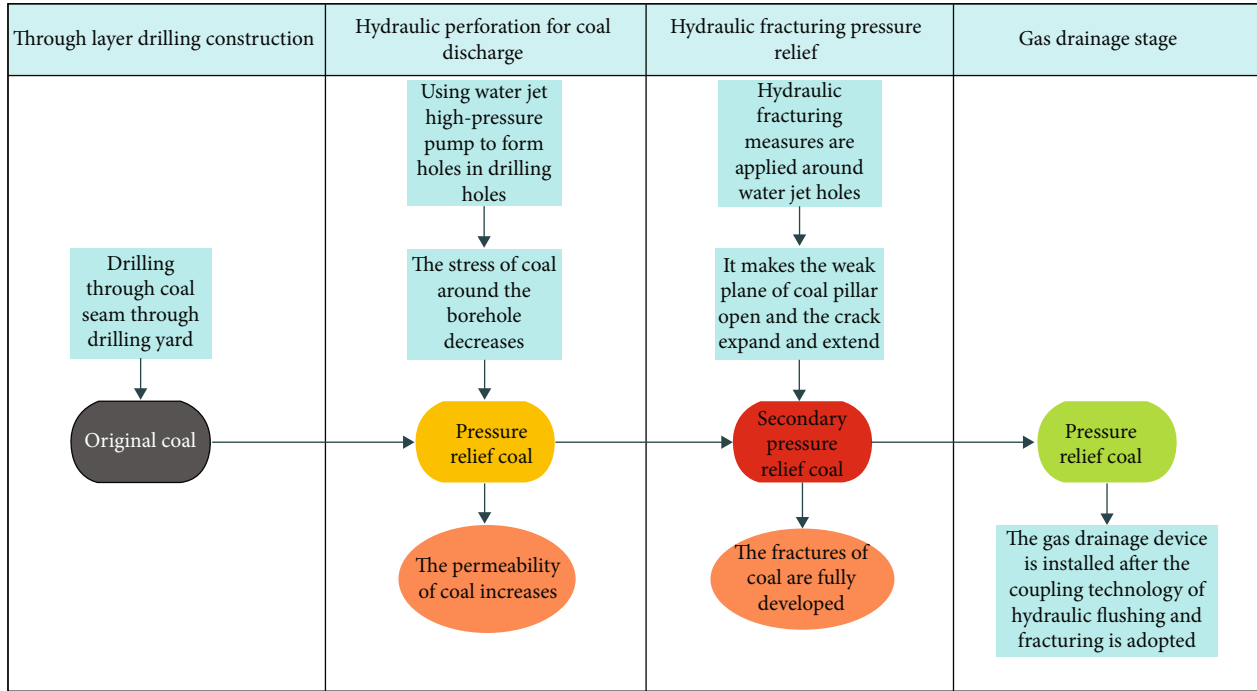


FIGURE 3: Working diagram of hydraulic flushing coal drainage and fracturing coupling fracturing and permeability enhancement technology.

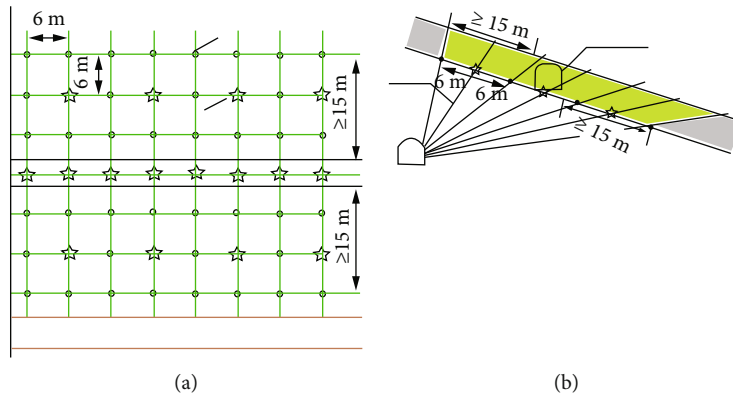


FIGURE 4: The layout of hydraulic perforation and hydraulic fracturing drilling. (a) The whole and (b) the local.

TABLE 1: Physical and mechanical parameters.

Stratum	Thickness (m)	Density (KN/m ³)	Bulk modulus (GPa)	Shear modulus (GPa)	Cohesion (MPa)	Angle of internal friction (°)	Tensile strength (MPa)
Roof	6	24	45	11.3	3.6	21	3.8
Coal seam	6	14	0.2	0.04	0.8	19	0.32
Floor	6	24	35	9.5	4.2	28	5.2

distribution. (1) The coal stress around the hydraulic fracturing borehole has been reduced, and the stress distribution is uniform. There is no stress concentration between the boreholes. (2) After implementing hydraulic perforation measures, the stress in the coal was 0~0.5 MPa measured in a zone 0~0.45 m from the fracturing borehole. The stress in the coal was

0.5 MPa~3 MPa measured in a zone 0.45 m~2 m from the fracturing borehole. Finally, the stress in the coal was 3 MPa~3.5 MPa measured in a zone 2 m~3.5 m from the fracturing borehole. (3) The coal stress between the fracturing borehole and adjacent boreholes has been reduced. In addition, the stress is uniformly distributed and is not concentrated. The

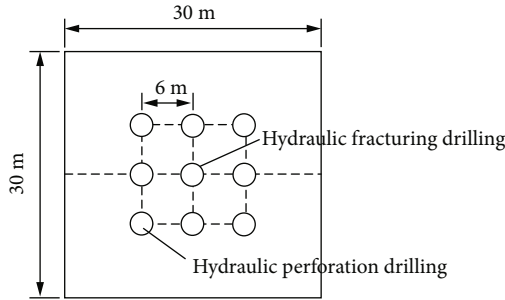


FIGURE 5: The drill hole layout of the numerical simulation scheme.

coal stress between boreholes is lower than the value before fracturing, which indicates that induced fractures passed through the concentrated stress coal pillars between the hydraulic perforation boreholes, promoting a uniform stress distribution in the coal.

3.3.2. Permeability Evolution. Figure 9 shows the coal permeability changes after hydraulic fracturing. After hydraulic fracturing, the coal permeability within a range of 2.5 m around the borehole reached 9×10^{-3} mD, representing an increase of approximately 3 times compared to the original coal permeability. Therefore, the coal cracks have formed a network around the hydraulic fracturing boreholes, resulting in a large area of coal pressure relief and increased permeability.

3.4. Analysis of Permeability Increment after Hydraulic Perforating and Fracturing. To compare the two measures, the stress and permeability data obtained using the value simulation calculation are subjected to statistical analysis. The curves of coal stress and permeability changes before and after implementing hydraulic fracturing measures in the No. 2₁ coal seam are shown in Figures 10 and 11.

The following observations can be made: (1) the coal stress around the boreholes is reduced, which indicates that both measures can reduce coal stress and improve coal permeability. (2) The magnitude of the stress decrease following hydraulic perforation is small. The coal stress is reduced within 1.5 m around the borehole. However, the coal stress increase between boreholes indicates that the coal between the boreholes experiences higher levels of stress. (3) The range of the stress reduction in the coal around the hydraulic fracturing borehole is far greater than that of the hydraulic perforation borehole, and the coal stress between the boreholes is significantly reduced, which indicates that hydraulic fracturing measures damage the coal between the hydraulic perforation boreholes and promote a significant decrease in coal stress between boreholes.

Figure 11 shows that hydraulic perforation caused an obvious increase in coal permeability within a 1.5 m wide zone around the borehole. The coal permeability within this zone increased by 1×10^{-3} mD on average compared to that of the original coal. The coal permeability within the zone 2.5 m~3.5 m from the borehole increased slightly, approximately 0.2×10^{-3} mD, compared to that of the original coal. Permeability-increasing technique that combines hydraulic perforation and hydraulic fracturing can significantly improve

coal permeability between boreholes. The coal permeability within 2 m of the hydraulic fracturing borehole increased by 8.5×10^{-3} mD on average compared to that of the original coal and increased by 7.0×10^{-3} mD compared to that of the hydraulic perforation borehole, which indicates that the permeability-increasing technique results in connections among the hydraulic fracturing boreholes. Consequently, a large area of decreased coal pressure and increased permeability develops through the elimination of the concentrated stress coal pillars between the hydraulic perforation boreholes.

4. Equipment and Process of the Permeability-Increasing Technique That Combines Hydraulic Perforation and Fracturing Coupling

The permeability-increasing hydraulic perforation and fracturing system is composed of a high-pressure feed pump, water tank, high-pressure pipes, hydraulic perforation blow-out control device, and other components. The connection sequence starting at the high-pressure water supply system is as follows: clean water pipe ($\Phi 108$ mm)→water tank (1.2 m^3)→high-pressure feed pump→high-pressure pipe→target layer borehole. The auxiliary equipment includes a pressure release valve, pressure gauge, flow meter, and other components. A schematic diagram of the permeability-increasing hydraulic perforation and fracturing system is shown in Figure 12. The water-gas separator and three-way device are shown in Figure 13.

The permeability-increasing process involving hydraulic perforation and fracturing is as follows: (1) use a drill bit 94 mm in diameter and provide positive pressure ventilation to create a hole in the coal seam. Stop using the drill rod, and expand the hole to 113 mm to prevent the drill hole from being blocked by pulverized coal. (2) Use a drill bit 133 mm in diameter to drill to a depth of 2.5 m. Inject polyurethane, fix the borehole orifice pipe, and connect it to a blowout control device with flanges. (3) Use a drill bit 75 mm in diameter to dig to the roof layer of the coal seam. Replace the drill bit with the special drill bits used for hydraulic perforation, and complete several rounds of hydraulic perforation. (4) Use a static water pressure (4~5 MPa) for hydraulic perforation. By comparing the expected and actual amounts of coal exposed by a single borehole, determine whether the hydraulic perforation process should include a high-pressure pump. Use a high-pressure pump to enhance the water injection strength. Perform hydraulic perforation following the principle of “using low pressure first and then high pressure.” (5) Select the 9 adjacent hydraulic perforation boreholes, and use the middle borehole of the “田” pattern as the hydraulic fracturing borehole. Inject highly pressurized water at 20 MPa into this borehole, and observe the status of the coal slime water around the hydraulic fracturing borehole. Plug the first borehole showing coal slime water with a special hole packer until all 8 adjacent boreholes presenting coal slime water complete the hydraulic fracturing process. (6) Remove the hole packers from the 9 boreholes to drain the coal slime water naturally. Use a drilling machine to penetrate the roof layer of the coal seam. (7) Seal

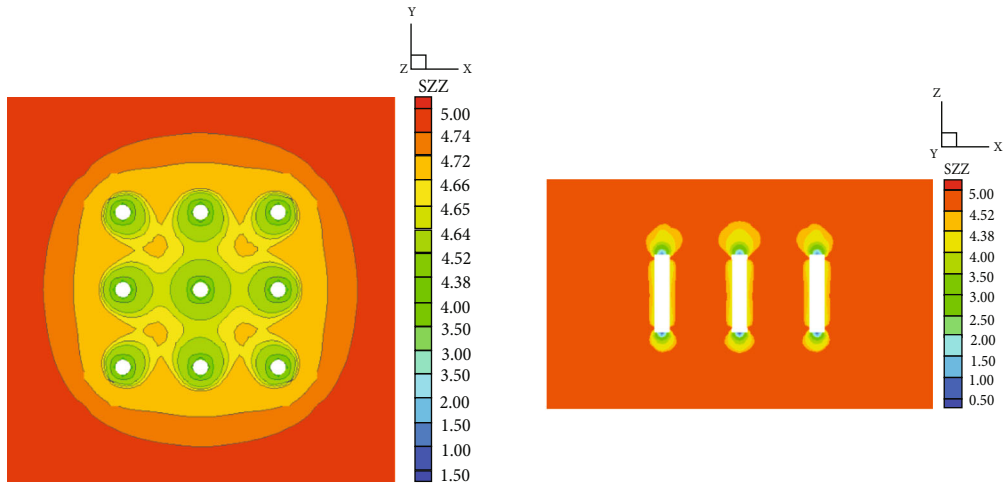


FIGURE 6: Stress field distribution diagram of horizontal and vertical profiles after hydraulic perforation.

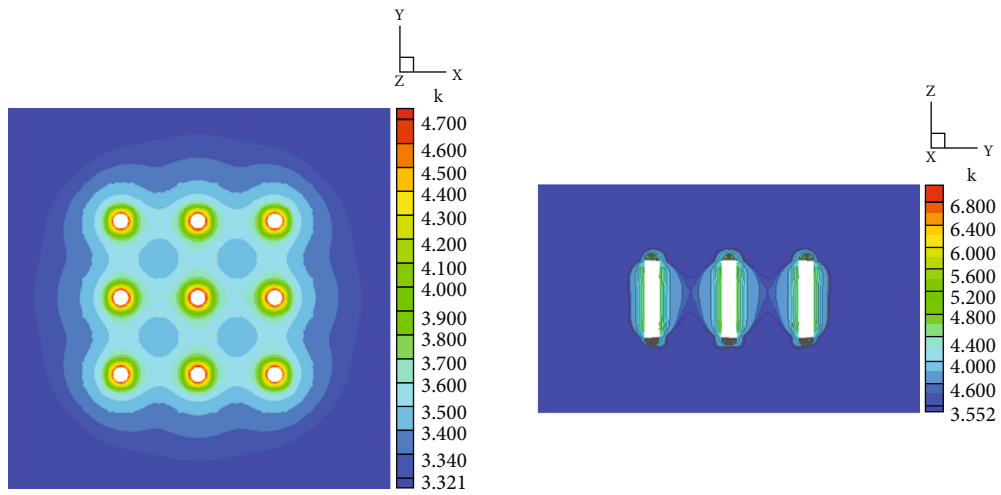


FIGURE 7: Permeability changes in horizontal and vertical profiles after hydraulic perforation.

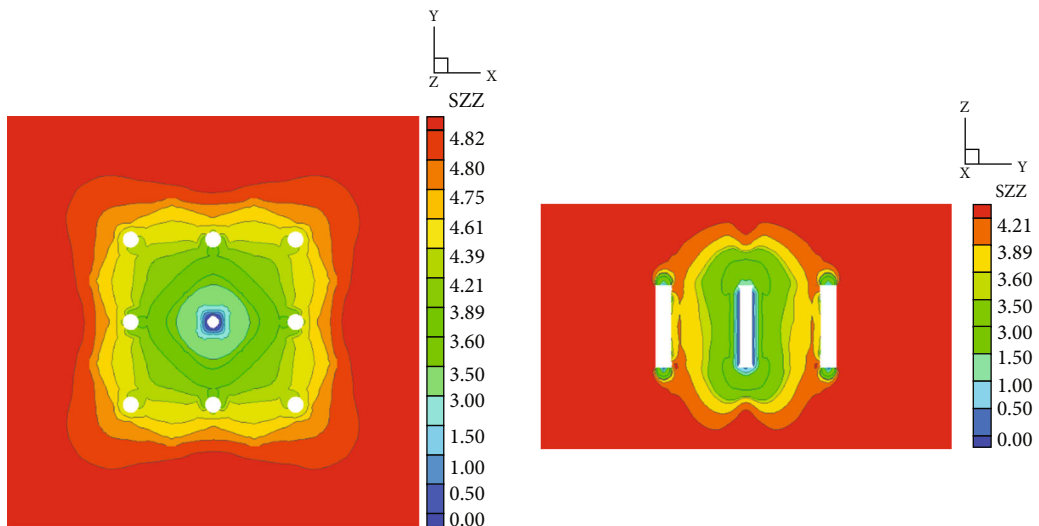


FIGURE 8: Stress field distribution of the horizontal and vertical profiles after hydraulic fracturing.

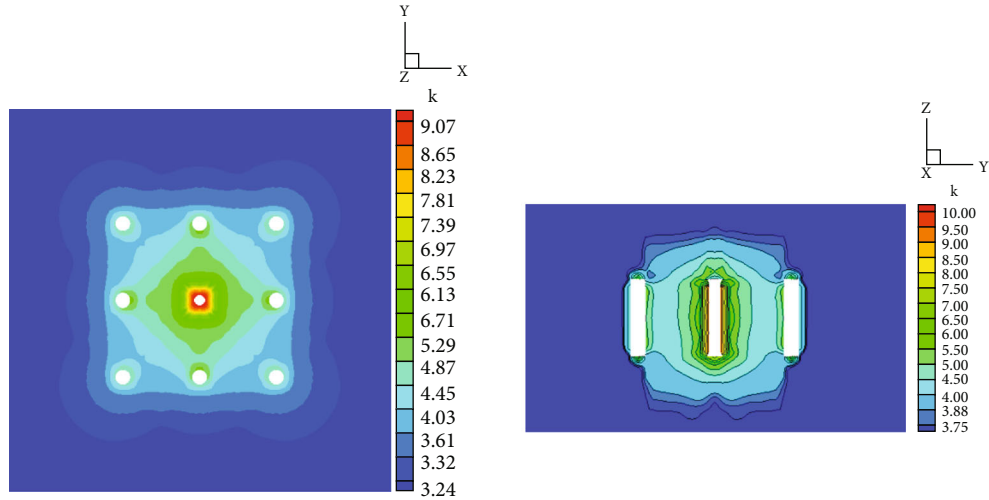


FIGURE 9: Permeability changes in the horizontal and vertical profiles after hydraulic fracturing.

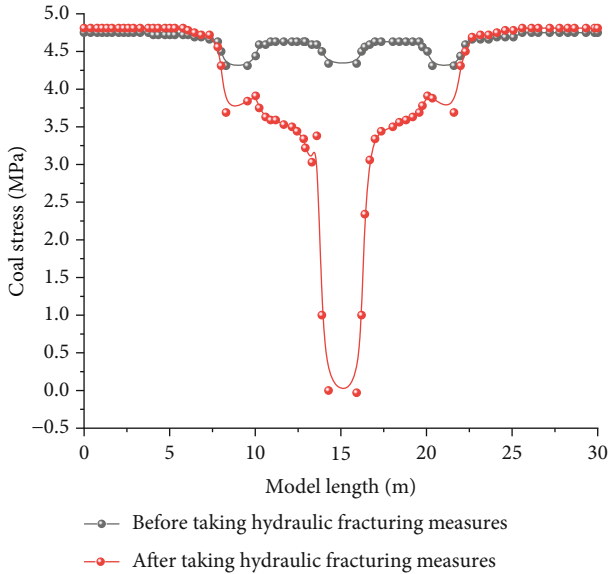


FIGURE 10: Curves of coal stress changes before and after implementing hydraulic fracturing measures.

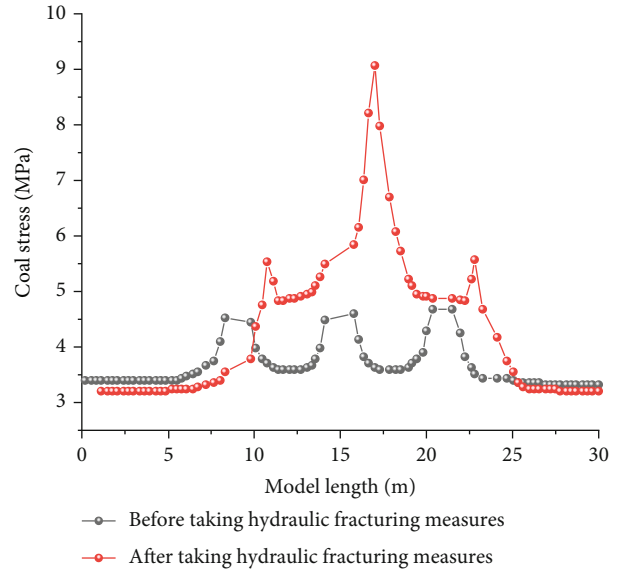


FIGURE 11: Curve of coal permeability changes before and after implementing hydraulic fracturing measures.

the borehole using two plugs and one injection. The hole sealing length should not be less than 8 m. Then, during extraction, treat the area as a single network.

5. On-Site Test of Hydraulic Perforation and Fracturing

5.1. *Basic Situation of the on-Site Test.* The 25091 coal face of the Zhengzhou Gaocheng mine was selected as the field test site. During the floor roadway construction process, 67 construction boreholes were drilled to measure the 6 m thickness of the No. 2₁ coal seam, which dips at an angle of 14°. The original measured gas content of the No. 2₁ coal seam was 7.45 m³/t~15.96 m³/t. The original gas pressure of the coal seam was 1.1 MPa, and the firmness coefficient of the coal seam was

0.2. The initial speed of the gas emission, ΔP , was 31. The type of coal destruction was characterized as types IV and V. The permeability coefficient of the coal seam was 0.0029 mD. In addition, the flow attenuation coefficient of the borehole, β , was 0.55~2.25 d⁻¹. In conclusion, the No. 2₁ coal seam of the 25091 coal face is characterized by a low permeability and a high likelihood of gas outbursts.

5.2. *Layout of Hydraulic Perforation and Hydraulic Fracturing Boreholes.* A row of boreholes at an interval of 6 m was established along the transportation roadway of the 25091 coal face. Seven hydraulic perforation boreholes were arranged in this row. While executing the hydraulic perforation, the workers controlled the amount of coal uncovering by regulating the water pressure of the hydraulic perforation. The amount of

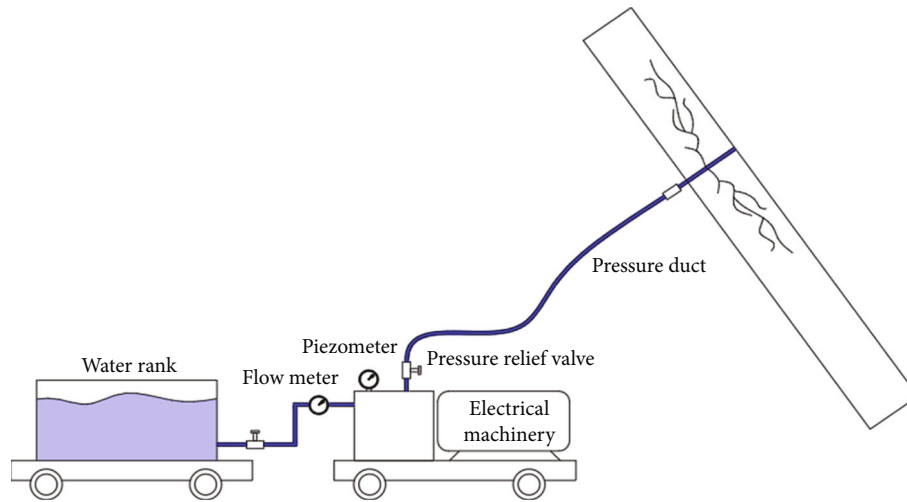


FIGURE 12: Schematic diagram of the hydraulic perforation and fracturing permeability-increasing system.

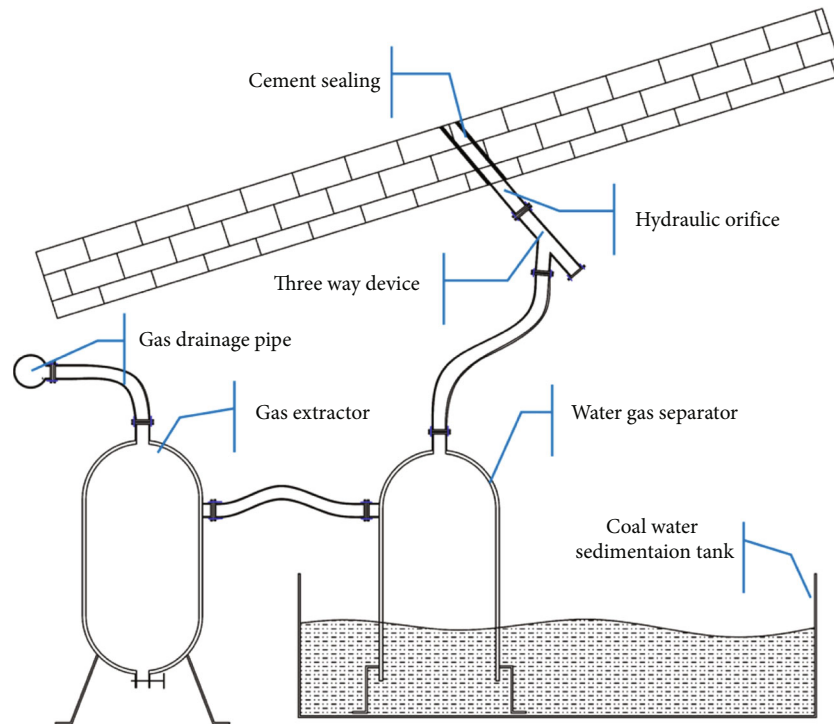


FIGURE 13: Water-gas separator and three-way device.

coal uncovering was checked using a special tool. The magnitude of coal uncovering should be no lower than 30%. The amount of coal uncovering in a single borehole should not be less than 7 tons. In addition, the amount of coal uncovering along each meter of coal borehole should not be less than 1 ton. After the amount of coal uncovering reached the given requirements, the workers performed hydraulic fracturing.

A set of boreholes was drilled per every 9 crossing holes into the floor drainage roadway. A hydraulic fracturing borehole for each group was created. The workers stopped fracturing when coal slime water appeared around the hydraulic fracturing borehole. The workers observed the hydraulic frac-

turing site, blocked each borehole with coal slime water with a special hole packer, and continued this process until all boreholes in the group presented coal slime water, indicating that the hydraulic fracturing of the group of boreholes had been completed. Then, the workers removed the coal slime from the boreholes and sealed the boreholes for linked extraction. The layout of the hydraulic perforation boreholes and hydraulic fracturing boreholes is shown in Figure 14.

5.3. Analysis of Gas Extraction and Outburst Elimination Effect. Hydraulic perforation measures were used only in the 25091 ventilation roadway of the Gaocheng mine; no hydraulic

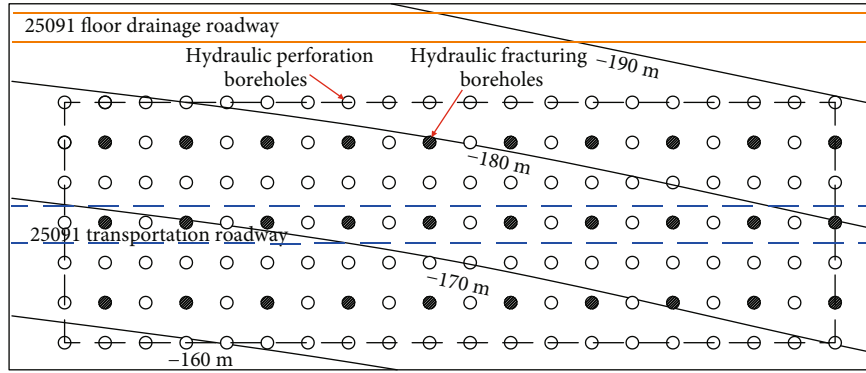


FIGURE 14: The layout of the hydraulic perforation and hydraulic fracturing boreholes.

fracturing was implemented. During the excavation process of the 25091 ventilation roadway, numerous hydraulic perforation boreholes with diameters ranging from 200 mm to 800 mm were created. In the vicinity of the hydraulic perforation boreholes, the outburst prediction index q was found to exceed the standard value, and the gas concentration of the return current increased. The analysis has shown that the volume of the effective permeability increase due to hydraulic perforation is small. In addition, the coal permeability just 3 m from the hydraulic perforation boreholes is quite poor, leading to stress concentration and enhanced outburst hazard. Therefore, in addition to hydraulic perforation, hydraulic fracturing should be applied to the 25091 transportation roadway to realize a large area of decreased pressure and increased permeability in the No. 2₁ coal seam.

5.3.1. Gas Extraction Effect. The gas conditions of the 25091 ventilation roadway and the 25091 transportation roadway at the Gaocheng mine are basically the same. Conventional permeability-increasing measures were used on the 25091 ventilation roadway. The magnitude of the coal uncovering via hydraulic perforation was 30%. Hydraulic fracturing measures and hydraulic perforation measures were used on the 25091 transportation roadway.

The extraction parameters of the lower #2 orifice, lower #8 orifice, and lower #18 orifice plate flow meters of the 25091 transportation bottom drainage roadway were compared to those of the upper #11 orifice, upper #22 orifice, and upper #43 orifice plate flow meters of the same roadway. The extracted gas concentrations before and after implementing hydraulic fracturing measures are shown in Figure 15.

The negative extraction pressure of the orifice plate flow meters of the 25091 transportation roadway was 31~37 MPa; the extracted gas concentration was 40%~91%; and the average rate of pure gas extraction from a single borehole was 0.12 m³/min during a consecutive 2~3 months of extraction. For the 25091 ventilation roadway, the negative extraction pressure of the orifice plate flow meters was 30.8~33.9 kPa; the extracted gas concentration was 4.8%~22.4%; and the average rate of pure gas extraction from a single borehole was 0.06 m³/min during a consecutive 2~3 months of extraction.

Figure 15 shows that, after adopting permeability-increasing hydraulic perforation measures, the average extracted gas concentration at 3 measuring points along the 25091 ventilation roadway

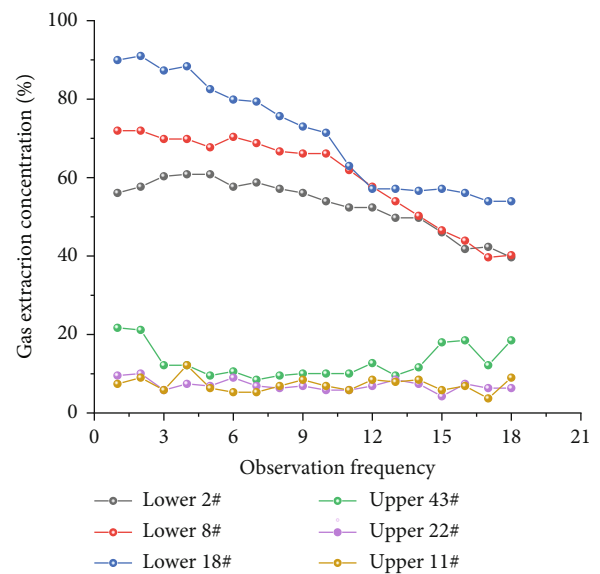


FIGURE 15: Extracted gas concentration before and after implementing hydraulic fracturing measures.

reached 9.3% with little variation. Following the hydraulic perforation, hydraulic fracturing measures were used on the 25091 transportation roadway. The induced fractures passed through the coal pillars between the hydraulic perforation boreholes. The average extracted gas concentration at 3 observation sites along the 25091 transportation roadway was 61.3%. In addition, the duration of the high-concentration gas extraction was long. The average extracted gas concentration of the transportation roadway was 6 times that of the ventilation roadway, demonstrating that the combination of hydraulic perforation and fracturing can significantly improve gas extraction, prolong borehole gas extraction duration, and achieve a large area of pressure relief and permeability increase in a coal seam, as well as efficient extraction of a coal seam.

5.3.2. Outburst Elimination Effect. A total of 672 boreholes were constructed in the 25091 transportation roadway, with an actual coal leakage magnitude of 32.8%. The actual extracted gas was 1,067,000 m³. In addition, the extraction percentage was 36%. The measured residual coal seam content

was $2.95 \text{ m}^3/\text{t} \sim 5.6 \text{ m}^3/\text{t}$. The measured residual gas pressure of the coal seam was $0.10 \text{ MPa} \sim 0.41 \text{ MPa}$, which was lower than the threshold values stipulated in the “coal and gas outburst prevention and control regulations” and the requirements of Henan Province. The regional outburst prevention measures have eliminated the outburst hazards of the No. 2₁ coal seam. During excavation of the 25091 transportation roadway, the workers collected coal samples to determine the initial speed from borehole gas emission, q , and drill cutting chips, S , to complete an outburst prediction for the working surface. The maximum measured outburst prediction index q value was $1.16 \text{ L}/\text{min}$, and the maximum value of S was $2.9 \text{ kg}/\text{m}$, both of which are less than the critical values stipulated in the “coal and gas outburst prevention and control regulations.” During excavation of the 25091 transportation roadway, the gas concentration of the return current was $0.01 \sim 0.52\%$, and the gas emission rate was $0.04 \sim 1.76 \text{ m}^3/\text{min}$. No dynamic hazard related to coal and gas outbursts was detected during the roadway excavation, demonstrating that permeability-increasing technique combining hydraulic perforation and hydraulic fracturing can effectively eliminate the outburst hazard of the No. 2₁ coal seam.

6. Conclusions

Aiming at the geological conditions of the soft three-layer low-permeability coal seam, this paper develops a new technology of enhanced permeability fracturing that combines hydraulic perforation and hydraulic fracturing. Numerical simulation studies the impact of this technology on the stress distribution and permeability of the coal seam around the borehole and investigates the concentration and volume of extracted borehole gas from multiple locations for comparative analysis. The conclusions are as follows:

- (1) The technical processes and parameters of increasing permeability via fracturing have been determined through a test combining hydraulic perforation and hydraulic fracturing in the Zhengzhou mining area. That is, “9-hole trellis hole arrangement method” is adopted. Firstly, hydraulic perforation and permeability-increasing technology is used in the surrounding 8 coal drainage boreholes, and then, the hydraulic fracturing permeability-increasing technology is used in the middle pressure relief hole
- (2) The permeability-increasing fracturing technique combining hydraulic perforation and hydraulic fracturing was adopted, and a large area of decreased pressure and increased permeability was achieved in the No. 2₁ coal seam in the Zhengzhou Gaocheng mine. The technique reduced the coal stress within the zone with fracture-induced increased permeability by 30%, increased the permeability by 3 times, and improved the average extracted gas concentration by more than 6 times. The gas pressure in the No. 2₁ coal seam decreased from 1.1 MPa to 0.4 MPa , and the gas content decreased from $15.96 \text{ m}^3/\text{t}$ to $5.6 \text{ m}^3/\text{t}$. During the coal roadway excavation process, the gas concentration of the return current was $0.01 \sim 0.52\%$. The

technique not only resulted in efficient gas extraction but also eliminated the dynamic hazards caused by coal and gas outbursts

- (3) Hydraulic fracturing measures should be performed after hydraulic perforation to form a large area of decreased pressure and increased permeability in the low-permeability coal seam. And the research results not only solve the problem of poor gas drainage effect in Gaocheng coal mine but also solve the problem of gas control in “three soft low-permeability outburst coal seam,” realize gas efficient drainage under the same geological conditions, realize “three soft low-permeability” coal seam gas efficient drainage in western Henan, and eliminate the dynamic hazards caused by coal and gas outbursts

Data Availability

The data used to support the findings of this study are included within the article.

Conflicts of Interest

The authors declare that they have no known competing financial interests or personal relationships that could have appeared to influence the work reported in this paper.

Authors' Contributions

Zhengjie Shang and Zhaofeng Wang conceived the experiment and analyzed the results; Zhiheng Cheng, Hongbing Wang, Liang Chen, Jianhua Fu, and Liu Hao coordinated the study and helped draft the manuscript. All authors gave final approval for publication.

Acknowledgments

The authors acknowledge the financial support provided by the National Natural Science Foundation of China (52074120) and the Fundamental Research Funds for the Central Universities (3142019005 and 3142017107).

References

- [1] D. Liu, J. Xu, G. Z. Yin, W. Z. Wang, Y. Q. Liang, and S. J. Peng, “Development and application of multifield coupling testing system for dynamic disaster in coal mine,” *Chinese Journal of Rock Mechanics and Engineering*, vol. 32, no. 5, pp. 966–975, 2013.
- [2] Q. Zou, T. Zhang, Z. Cheng, Z. Jiang, and S. Tian, “A method for selection rationality evaluation of the first-mining seam in multi-seam mining,” *Geomechanics and Geophysics for Geo-Energy and Geo-Resources*, vol. 8, no. 1, p. 17, 2022.
- [3] Z. H. Li, E. Y. Wang, J. C. Ou, and Z. Liu, “Hazard evaluation of coal and gas outbursts in a coal-mine roadway based on logistic regression model,” *International Journal of Rock Mechanics and Mining Sciences*, vol. 80, pp. 185–195, 2015.
- [4] T. C. Zhang, Q. L. Zou, X. Q. Jia, C. Z. Jiang, and X. G. Niu, “Effect of SiO_2 nanofluid with different concentrations on the wettability of coal,” *Fuel*, vol. 321, p. 124041, 2022.

- [5] C. J. Fan, S. Li, M. K. Lou, W. Z. Du, and Z. H. Yang, "Coal and gas outburst dynamic system," *International Journal of Rock Mechanics and Mining Sciences*, vol. 26, no. 6, pp. 75–82, 2016.
- [6] T. C. Zhang, Q. L. Zou, X. Q. Jia et al., "Effect of cyclic water injection on the wettability of coal with different SiO₂ nanofluid treatment time," *Fuel*, vol. 321, p. 122922, 2022.
- [7] A. T. Zhou, M. Zhang, K. Wang, and D. Elsworth, "Near-source characteristics of two-phase gas–solid outbursts in roadways," *International Journal of Coal Science & Technology*, vol. 8, no. 4, pp. 685–696, 2021.
- [8] Y. P. Liang, Q. C. Ran, Q. L. Zou, B. C. Zhang, and Y. Hong, "Experimental study of mechanical behaviors and failure characteristics of coal under true triaxial cyclic loading and unloading and stress rotation," *Natural Resources Research*, vol. 31, no. 2, pp. 971–991, 2022.
- [9] A. Liu, S. M. Liu, P. Liu, and K. Wang, "Water sorption on coal: effects of oxygen-containing function groups and pore structure," *International Journal of Coal Science & Technology*, vol. 8, no. 5, pp. 983–1002, 2021.
- [10] Q. L. Zou, T. C. Zhang, T. F. Ma, S. X. Tian, X. Q. Jia, and Z. B. Jiang, "Effect of water-based SiO₂ nanofluid on surface wettability of raw coal," *Energy*, vol. 254, p. 124228, 2022.
- [11] S. B. Chen, C. Zhang, X. Y. Li, Y. Zhang, and X. Wang, "Simulation of methane adsorption in diverse organic pores in shale reservoirs with multi-period geological evolution," *International Journal of Coal Science & Technology*, vol. 8, no. 5, pp. 844–855, 2021.
- [12] Q. Zou, H. Liu, Z. Jiang, and X. Wu, "Gas flow laws in coal subjected to hydraulic slotting and a prediction model for its permeability-enhancing effect," *Energy Sources, Part A: Recovery, Utilization, and Environmental Effects*, pp. 1–15, 2021.
- [13] B. Jiang, Y. Qin, Y. W. Ju, J. L. Wang, and M. Li, "The coupling mechanism of the evolution of chemical structure with the characteristics of gas of tectonic coals," *Earth Science Frontiers*, vol. 16, no. 2, pp. 262–271, 2009.
- [14] T. Liu, B. Q. Lin, X. H. Fu, and A. Liu, "Mechanical criterion for coal and gas outburst: a perspective from multiphysics coupling," *International Journal of Coal Science & Technology*, vol. 8, no. 6, pp. 1423–1435, 2021.
- [15] M. H. Yi, L. Wang, C. M. Hao, Q. Q. Liu, and Z. Y. Wang, "Method for designing the optimal sealing depth in methane drainage boreholes to realize efficient drainage," *International Journal of Coal Science & Technology*, vol. 8, no. 6, pp. 1400–1410, 2021.
- [16] X. L. Li, S. J. Chen, Q. M. Zhang, X. Gao, and F. Feng, "Research on theory, simulation and measurement of stress behavior under regenerated roof condition," *Geomechanics and Engineering*, vol. 26, no. 1, pp. 49–61, 2021.
- [17] X. L. Li, S. J. Chen, and S. Wang, "Study on in situ stress distribution law of the deep mine taking Linyi mining area as an example," *Advances in Materials Science and Engineering*, vol. 9, Article ID 5594181, 2021.
- [18] X. Wang, Z. M. Xu, Y. J. Sun, J. M. Zheng, C. H. Zhang, and Z. W. Duan, "Construction of multi-factor identification model for real-time monitoring and early warning of mine water inrush," *International Journal of Mining Science and Technology*, vol. 31, no. 5, pp. 853–866, 2021.
- [19] L. Jia, K. W. Li, X. H. Shi, L. P. Zhao, and J. S. Linghu, "Application of gas wettability alteration to improve methane drainage performance: a case study," *International Journal of Mining Science and Technology*, vol. 31, no. 4, pp. 621–629, 2021.
- [20] H. J. Guo, K. Wang, Y. C. Wu et al., "Evaluation of the weakening behavior of gas on the coal strength and its quantitative influence on the coal deformation," *International Journal of Mining Science and Technology*, vol. 31, no. 3, pp. 451–462, 2021.
- [21] Z. W. Wang, Y. Qin, T. Li, and X. Y. Zhang, "A numerical investigation of gas flow behavior in two-layered coal seams considering interlayer interference and heterogeneity," *International Journal of Mining Science and Technology*, vol. 31, no. 4, pp. 699–716, 2021.
- [22] Q. Y. Tu, Y. P. Cheng, S. Xue, T. Ren, and X. Cheng, "Energy-limiting factor for coal and gas outburst occurrence in intact coal seam," *International Journal of Mining Science and Technology*, vol. 31, no. 4, pp. 729–742, 2021.
- [23] X. L. Li, S. J. Chen, S. M. Liu, and Z. H. Li, "AE waveform characteristics of rock mass under uniaxial loading based on Hilbert-Huang transform," *Journal of Central South University*, vol. 28, no. 6, pp. 1843–1856, 2021.
- [24] W. G. Zhao, J. R. Wang, T. W. Lan, J. Z. Sun, Q. Li, and C. S. Li, "Permeability test and gas drainage technology of low permeability coal seam," *Journal of Liaoning Technical University (Natural Science)*, vol. 39, no. 3, pp. 201–207, 2020.
- [25] W. Qiao, Q. Jiang, and R. Jian, "Optimization study on double gas drainage system of low permeability thick seam," *Coal Science and Technology*, vol. 41, no. 2, pp. 45–48, 2013.
- [26] Y. J. Zhao, S. R. Xie, B. G. Wen, H. D. Guo, and S. J. Yuan, "Gas drainage technique by 1 000 m long and large diameter roof boreholes in high gas coal seam group," *Journal of China Coal Society*, vol. 34, no. 6, pp. 797–801, 2009.
- [27] H. B. Wang, T. Li, Q. L. Zou, Z. H. Cheng, and Z. K. Yang, "Influences of path control effects on characteristics of gas migration in a coal reservoir," *Fuel*, vol. 267, p. 117212, 2020.
- [28] Z. F. Wang, Y. C. Fan, and S. S. Li, "Application of borehole hydraulic flushing technology to soft and outburst seam with low permeability," *Coal Science and Technology*, vol. 40, no. 2, pp. 52–55, 2012.
- [29] H. W. Zhang, X. Fu, B. J. Huo, Y. B. Lu, and K. Y. Zhou, "Experimental study on the pressure-relief effect of the protective seam mining at low permeability seam mining at low permeability seam," *Journal of Safety and Environment*, vol. 17, no. 6, pp. 2134–2139, 2017.
- [30] G. Cui, "Permeability improved technology of low permeability seams group in underground mine," *Coal Science and Technology*, vol. 44, no. 5, pp. 151–154, 2016.
- [31] X. Cheng, G. M. Zhao, Y. M. Li et al., "Evolution of overburden mining-induced fractured zone and pressure-relief gas drainage in soft rock protective seam," *Journal of Mining & Safety Engineering*, vol. 37, no. 3, pp. 533–542, 2020.
- [32] H. B. Wang, Z. H. Cheng, T. Li et al., "Evolution characteristics of a high-level asymmetric fracture-seepage community and precise coalbed methane drainage technology during mining of outburst-prone coal seam groups," *Shock and Vibration*, vol. 1, no. 14, Article ID 5537909, 2021.
- [33] Q. L. Zou, H. Liu, Y. J. Zhang, Q. M. Li, J. W. Fu, and Q. T. Hu, "Rationality evaluation of production deployment of outburst-prone coal mines: a case study of Nantong coal mine in Chongqing, China," *Safety Science*, vol. 122, p. 104515, 2020.
- [34] X. Bai, D. M. Zhang, S. Zeng, S. Zhang, D. Wang, and F. Wang, "An enhanced coalbed methane recovery technique based on

- CO₂ phase transition jet coal-breaking behavior,” *Fuel*, vol. 265, p. 116912, 2020.
- [35] D. M. Zhang, X. Bai, G. Z. Yin, Z. Rao, and Q. B. He, “Research and application on technology of increased permeability by liquid CO₂ phase change directional jet fracturing in low-permeability coal seam,” *Journal of China Coal Society*, vol. 43, no. 7, pp. 1938–1950, 2018.
- [36] G. Z. Yin, B. Z. Deng, M. H. Li et al., “Impact of injection pressure on CO₂-enhanced coalbed methane recovery considering mass transfer between coal fracture and matrix,” *Fuel*, vol. 196, pp. 288–297, 2017.
- [37] Z. Y. Ti, F. Zhang, J. Pan, X. Ma, and Z. Shang, “Permeability enhancement of deep hole pre-splitting blasting in the low permeability coal seam of the Nanting coal mine,” *PLoS One*, vol. 13, no. 6, article e0199835, 2018.
- [38] J. Liu, Z. G. Liu, K. Gao, and W. Zhou, “Application of deep hole pre-splitting blasting to gas drainage at deep well and low permeability coal seam,” *Journal of Safety Science and Technology*, vol. 10, no. 5, pp. 148–153, 2014.
- [39] Y. P. Liang, Y. T. Tan, F. K. Wang, Y. J. Luo, and Z. Q. Zhao, “Improving permeability of coal seams by freeze-fracturing method: the characterization of pore structure changes under low-field NMR,” *Energy Reports*, vol. 6, pp. 550–561, 2020.
- [40] E. Y. Wang, H. Wang, X. F. Liu, X. Shen, and C. L. Zhang, “Spatio temporal evolution of geostress and gas field around hydraulic punching borehole in coal seam,” *Coal Science and Technology*, vol. 48, no. 1, pp. 39–45, 2020.
- [41] D. Liu and W. Liu, “Research on gas extraction technology: hydraulic stamping hydrofracture to pressure relief and permeability improvement,” *Coal Science and Technology*, vol. 47, no. 3, pp. 136–141, 2019.
- [42] Y. Q. Tao, C. L. Zhang, J. Xu, S. J. Peng, and D. Feng, “Effect evaluation on pressure relief and permeability improvement of hydraulic flushing physical experiment,” *Journal of Chongqing University*, vol. 41, no. 10, pp. 69–77, 2018.
- [43] Q. L. Zou and B. Q. Lin, “Fluid–solid coupling characteristics of gas-bearing coal Subjected to hydraulic slotting: an experimental investigation,” *Energy & Fuels*, vol. 32, no. 2, pp. 1047–1060, 2018.
- [44] K. G. Zheng, “Permeability improving technology by sectional hydraulic fracturing for comb-like long drilling in floor of crushed and soft coal seam with low permeability,” *Journal of Mining & Safety Engineering*, vol. 37, no. 2, pp. 272–281, 2020.
- [45] W. Yang, C. Z. Lu, G. Y. Si, B. Lin, and X. Jiao, “Coal and gas outburst control using uniform hydraulic fracturing by destress blasting and water-driven gas release,” *Journal of Natural Gas Science and Engineering*, vol. 79, p. 103360, 2020.
- [46] Q. L. Zou, H. Liu, Z. H. Cheng, T. C. Zhang, and B. Q. Lin, “Effect of slot inclination angle and borehole-slot ratio on mechanical property of pre-cracked coal: implications for ECBM recovery using hydraulic slotting,” *Natural Resources Research*, vol. 29, no. 3, pp. 1705–1729, 2020.